Topological thermoelectric effects in spin-orbit coupled electron- and hole-doped semiconductors

E. Dumitrescu, Chuanwei Zhang, D. C. Marinescu, and Sumanta Tewari

Phys. Rev. B **85**, 245301 — Published 1 June 2012

DOI: 10.1103/PhysRevB.85.245301

Topological thermoelectric effects in spin-orbit coupled electron and hole doped semiconductors

E. Dumitrescu[1], Chuanwei Zhang[2], D. C. Marinescu[1], and Sumanta Tewari[1]
[1]*Department of Physics and Astronomy, Clemson University, Clemson, SC 29634 USA*
[2]*Department of Physics and Astronomy, Washington State University, Pullman, WA 99164 USA*

We compute the intrinsic contributions to the Berry-phase mediated anomalous Hall and Nernst effects in electron- and hole-doped semiconductors in the presence of an in-plane magnetic field as well as Rashba and Dresselhaus spin orbit couplings. For both systems we find that the regime of chemical potential which supports the topological superconducting state in the presence of superconducting proximity effect can be characterized by plateaus in the topological Hall and Nernst coefficients flanked by well-defined peaks marking the emergence of the topological regime. The plateaus arise from a clear momentum space separation between the region where the Berry curvature is peaked (at the 'near-band-degeneracy' points) and the region where the single (or odd number of) Fermi surface lies in the Brillouin zone. The plateau for the Nernst coefficient is at vanishing magnitudes surrounded by two large peaks of opposite signs as a function of the chemical potential. These results could be useful for experimentally deducing the chemical potential regime suitable for realizing topological states in the presence of proximity effect.

I. INTRODUCTION

Topological superconducting states with or without broken time-reversal symmetry[1–3] have recently come under increasing attention because of the possibility of realizing Majorana fermions. Majorana fermions,[4–11] defined by self-hermitian second quantized operators $\gamma = \gamma^\dagger$, are remarkable quantum mechanical particles which can be construed as their own anti-particles. Recently it has been shown that a 2D electron-doped semiconductor with Rashba type spin-orbit coupling in proximity to a bulk s-wave superconductor and an externally induced perpendicular Zeeman splitting can support a topological superconducting phase with Majorana fermion modes at vortex cores and sample edges.[12–14] The proposal followed on an earlier similar proposal for topological superconducting states using spin-orbit coupling and Zeeman fields made in the context of cold fermions.[15,16] It has also been pointed out by Alicea[17] that in the presence of Dresselhaus spin-orbit coupling co-existing along with the usual Rashba coupling, the topological superconducting state in electron-doped semiconductors can be realized with an in-plane Zeeman field. Since the in-plane Zeeman field can be directly applied by an in-plane magnetic field which is free of the orbital effects, the geometry proposed by Alicea is useful for producing topological superconductivity in two-dimensional electron systems. Very recently it has also been shown[18] that the generic Luttinger Hamiltonian applicable to the hole-doped semiconductors also supports topological superconductivity and Majorana fermions in the presence of a perpendicular Zeeman field in a manner similar to its electron-doped counterpart. The possibility of a larger value of the effective mass and spin-orbit coupling in p-type holes in a semiconductor quantum well makes the hole-doped systems an attractive candidate for realizing topological superconductivity that breaks time-reversal symmetry. The strategy of producing topological superconductivity and Majorana fermions using Rashba spin-orbit coupling, parallel Zeeman field, and s-wave superconductivity has also been applied to electron- and hole-doped one dimensional semiconducting wires.[14,19–21] The one dimensional topological systems are particularly useful for constructing quasi-two-dimensional quantum wire networks[22] which can potentially be used[22–24] as platforms for non-Abelian statistics[6–9] and universal quantum computation[10,11] in the Bravyi-Kitaev scheme.[25] For the purpose of studying anomalous topological transverse response functions such as anomalous Hall and Nernst effects, in this paper we will confine ourselves to two-dimensional hole- and electron-doped semiconductor thin films.

The substantive difference between the topological states in the electron and hole doped semiconductors lies in the fact that while the superconducting order parameter in the former is similar to the chiral p-wave $(p_x + ip_y)$ type, the order parameter in the hole-doped system in a perpendicular Zeeman field is predominantly chiral f-wave $(f_x + if_y)$ type.[18] A strong perpendicular Zeeman field, however, is difficult to realize experimentally with a magnetic field because of the unwanted orbital effects which are pair breaking.[17] Following Ref. [17], in this paper we will introduce the geometry and Hamiltonian for the hole-doped systems which can support topological superconductivity in the presence of an in-plane Zeeman field making it easier to produce with a magnetic field. We will then analyze the Berry phase mediated topological Hall and thermoelectric effects in electron- and hole-doped systems under external conditions necessary for realizing topological superconductivity with broken time-reversal symmetry. Note that, since we are considering the spontaneous or anomalous components of the Hall and Nernst effects, we will only treat two-dimensional systems in the presence of an *in-plane* Zeeman splitting.

In all the systems mentioned above the chemical potential regime that corresponds to the topological state in the presence of proximity effect is characterized by a

single (or odd number of) Fermi surface which breaks the fermion doubling theorem.[26] It has been argued that, in the limit of vanishing superconducting pair potential Δ_0, the single (or odd number) of Fermi surface at the chemical potential constitutes a necessary condition for the existence of topological superconductivity and Majorana fermions at order parameter defects.[27] The breakdown of the fermion doubling theorem and topological superconductivity in all the above cases are achieved by the introduction of a strong Zeeman splitting greater than at least the proximity induced superconducting pair potential Δ_0. At such high values of the Zeeman splitting the superconductivity itself survives because of the spin-chirality induced on the semiconductor Fermi surface by a strong enough spin-orbit coupling.[14]

The twin requirements of strong Zeeman splitting as well as spin-orbit coupling on the semiconductor Fermi surface manifest themselves in interesting Berry phase[28] mediated topological effects which have pronounced effects on the anomalous Hall and thermoelectric coefficients.[29–44] While these effects have been investigated previously, our focus in this paper is near the chemical potential regime - called topological regime hereafter - which supports topological superconductivity in the presence of s-wave proximity effect. We find that the topological regimes in both electron- and hole-doped semiconductors are marked by well-defined plateaus in the anomalous Hall and Nernst effects as a function of the chemical potential. The plateaus are not quantized, however, in the sense of quantized anomalous transport coefficients, because, even in the topological regime, the electron or the hole-doped systems are not fully gapped. Rather, in this regime of chemical potential they have a single (or odd number of) Fermi surface which supports, in the presence of spin-chirality induced by the spin-orbit coupling, the superconducting proximity effect. Even so, in the topological regime, there is a clear separation in the momentum space between the region where the Berry curvature is peaked (near the 'band-degeneracy' points in the absence of the Zeeman splitting) and the region where the Fermi surface lies in the Brillouin zone. Since the Nernst effect is strictly a Fermi surface quantity at zero temperature, the vanishing of the overlapping region in the Brillouin zone between the Fermi surface and the Berry curvature results in a vanishing anomalous Nernst effect in the topological regime. The plateau in the Nernst coefficient at vanishing magnitudes is flanked on either side of the topological regime by well-defined peaks (of opposite signs) arising from the emergence of a second small Fermi surface which destroys topological superconductivity but gives rise to large peaks in the topological Nernst effect. The results presented in this paper may be useful for experimentally deducing the topological regimes of the chemical potential in electron and hole-doped semiconductors supporting Majorana fermions in the presence of proximity effect.

II. BERRY PHASE AND TOPOLOGICAL HALL AND NERNST EFFECTS

As a particle moves adiabatically through a closed contour in its parameter space it acquires a geometric phase known as a Berry phase. In a crystal lattice the wavefunctions for a band are written as $|\Psi_n(\boldsymbol{k},\boldsymbol{r})\rangle = e^{i\boldsymbol{k}\cdot\boldsymbol{r}}\,|u_n(\boldsymbol{k},\boldsymbol{r})\rangle$ according to Bloch's theorem where $|u_n(\boldsymbol{k},\boldsymbol{r})\rangle$ is a Bloch function with the periodicity of the lattice. The eigenfucntions are k dependent and the relevant paramater space is the space defined by the crystal momentum $\mathbf{k}$. The Berry connection, $\boldsymbol{A_k} = \langle u_n(\boldsymbol{k},\boldsymbol{r})\,|i\nabla_{\boldsymbol{k}}|\,u_n(\boldsymbol{k},\boldsymbol{r})\rangle$ represents the geometric phase acquired by a Bloch wave function through infinitesimal movement in k-space and is a vector potential. In analogy to electrodynamics the Berry curvature is defined as the curl of this potential as $\boldsymbol{\Omega}_n(\boldsymbol{k}) = \nabla_{\boldsymbol{k}} \times \boldsymbol{A_k}$ which is Berry phase per unit area. The Berry curvature enters into the equations of motion of a wavepacket and is responsible for many intrinsic transport properties. For a system with time reversal symmetry and spatial inversion symmetry the Berry curvature vanishes for all $\mathbf{k}$ so it is often ignored.

The charge current in the presence of an electric field $\mathbf{E}$ and a temperature gradient ∇T can be written as $J_i = \sigma_{ij}E_j + \alpha_{ij}(\partial_j T)$ where σ_{ij} and α_{ij} are the electric and thermoelectric conductivity tensors. In the Hall effect a current is applied and a magnetic field is present perpendicular to a conducting sample. In this configuration an electric field is generated perpendicular to the current so that off diagonal terms of σ_{ij} are non-zero. Similarly for the Nernst effect a current will arise normal to the temperature gradient when a perpendicular magnetic field is present. Below we discuss the anomalous or topological Hall and Nernst effects for a system where there is no perpendicular magnetic field but there is still a contribution to the Hall and Nernst effects due to the presence of a non-trivial Berry curvature.

In the presence of an electric field $\mathbf{E}$, the group velocity of a Bloch electron is written as[30]

$$\dot{\boldsymbol{r}} = \frac{1}{\hbar}\frac{\partial \epsilon_n(\boldsymbol{k})}{\partial \boldsymbol{k}} + \frac{e}{\hbar}\mathbf{E} \times \boldsymbol{\Omega}_{\mathbf{n}}(\mathbf{k}) \tag{1}$$

where the first term is the usual band dispersion and the second term is called the anomalous velocity. This anomalous velocity is responsible for the intrinsic contribution to the anomalous Hall and anomalous Nernst effects, with the Berry curvature acting like a magnetic field in k-space. With the inclusion of the anomalous velocity it immediately follows that by summing the anomalous velocity over all occupied states the charge conductivity is written as,[33,34]

$$\sigma_{xy} = \frac{e^2}{\hbar}\sum_n \int \frac{dk_x dk_y}{(2\pi)^2}\Omega_n f(E_n(\boldsymbol{k})) \tag{2}$$

where $f(E_n) = 1/(1+\exp(E_n-\mu)/k_BT)$ is the Fermi

distribution function, k_B is the Boltzmann constant and T is the temperature.

In order to write an expression for the anomalous Nernst coefficient we first look at the coefficient $\bar{\alpha}_{xy}$ which relates the heat current and electric field by $J_x^h = \bar{\alpha}_{xy} E_y$. α_{xy} can then be solved for by making use of the Onsager relation $\bar{\alpha}_{xy} = T\alpha_{xy}$. The transverse heat coefficient may be written as the velocity multiplied by the entropy density,

$$\bar{\alpha}_{xy} = T\alpha_{xy} = \frac{e}{\beta\hbar}\sum_n \int \frac{dk_x dk_y}{(2\pi)^2}\Omega_n s_n(k), \qquad (3)$$

where the entropy density of an electron gas is given as $s(k) = -f_k \ln f_k - (1-f_k)\ln(1-f_k)$ with f_k as the Fermi distribution function. Using the above equation and this form for the entropy density, the coefficient α_{xy} may be re-written as:[33,34]

$$\alpha_{xy} = \frac{e}{\hbar}\frac{1}{T}\sum_n \int \frac{dk_x dk_y}{(2\pi)^2}\Omega_n \times \{E_n(\boldsymbol{k}) f(E_n(\boldsymbol{k})) - k_B T \log[1 - f(E_n(\boldsymbol{k}))]\}. \qquad (4)$$

Through the use of these Berry phase mediated thermoelectric effects one can characterize the topological regimes in chemical potentials which support the topological superconducting state in the presence of superconducting proximity effect. We will deliberately choose quantum well configurations with appropriate spin-orbit couplings which will allow an in-plane Zeeman field for the topological state so the conventional Hall and thermoelectric effects make no contributions in experiments.

III. TOPOLOGICAL HALL AND NERNST EFFECTS IN ELECTRON DOPED SEMICONDUCTORS

As a warm-up, following Alicea,[17] we first consider a zinc-blend semiconductor quantum well grown in the [110] direction with an in-plane magnetic field applied parallel to the semiconductor film. In such a quantum well we expect both Rashba and Dresselhaus spin orbit couplings to be present and the Hamiltonian of this system on the $(x-y)$ plane is written as,[17]

$$H = \frac{\hbar^2 k^2}{2m^*} + \alpha_R(\boldsymbol{\sigma}\times\boldsymbol{k})\cdot\hat{z} + \alpha_D k_x \sigma_z + h_y \sigma_y \qquad (5)$$

Here, α_R and α_D are the strengths of the Rashba and Dresselhaus couplings, m^* is the effective mass of the electrons, h_y the magnitude of the in-plane Zeeman field and the $\boldsymbol{\sigma} = (\sigma_x, \sigma_y, \sigma_z)$ are the Pauli matrices. Diagonalizing the Hamiltonian yields energy eigenvalues of $E_\pm = \frac{h^2k^2}{2m^*} + E_0$, where $E_0 = \sqrt{(\alpha_D k_x)^2 + (\alpha_R k_y)^2 + (\alpha_R k_x - h_y)^2}$. The degeneracy between the two bands is lifted by the presence of both Dresselhaus spin orbit coupling and the in-plane magnetic field. It is easy to see that, in the absence of the Dresselhaus coupling, the in-plane Zeeman splitting can be reabsorbed in the Hamiltonian by a re-definition of the momentum $\alpha_R k_x \to \alpha_R k_x + h_y$ which leaves the system gapless even with the Zeeman splitting. The existence of a non-zero Dresselhaus term α_D ensures that a finite gap is created near the band-degeneracy points at a non-zero value of k_x even after this re-definition. The minimum gap between the bands, $\Delta = 2\alpha_D h_y/\sqrt{\alpha_R^2 + \alpha_D^2}$, is located at $k_x = \alpha_R h_y/(\alpha_R^2 + \alpha_D^2)$ and $k_y = 0$,[44] which is shown in the inset of figure 2.

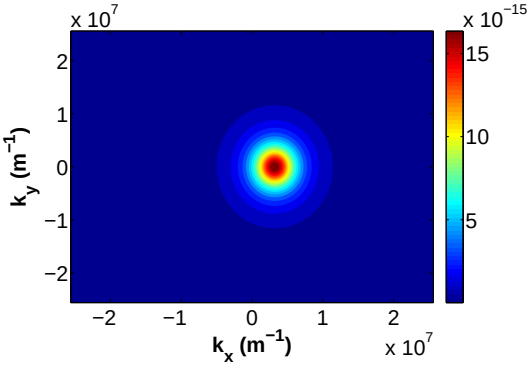

FIG. 1. Contour plot of the Berry curvature $\boldsymbol{\Omega}_-$ in the lower band of electron-doped semiconductors. The Berry curvature is sharply peaked at a finite value of k_x near the band-degeneracy point in the absence of the Dresselhaus coupling.

We calculate the Berry curvatures for this system through $\boldsymbol{\Omega}_\pm = 2\mathrm{Im}\left\langle \frac{\partial\Phi_\pm}{\partial k_x} \middle| \frac{\partial\Phi_\pm}{\partial k_y} \right\rangle \hat{z}$, where $\Phi\pm$ are the eigenstates of the Hamiltonian in Eq. (5). Evaluating this expression analytically we find that[44]

$$\boldsymbol{\Omega}_\pm = \mp\frac{\alpha_R \alpha_D h_y}{2E_0^3}\hat{z}, \qquad (6)$$

which are of equal magnitude and opposite signs in the two bands. In Fig. 1 we plot $\boldsymbol{\Omega}_-$ where it can be seen that the Berry curvature is sharply peaked at the gap minimum between the two bands, i.e., at the band degeneracy point in k-space in the absence of the Dresselhaus coupling. We note here that the Berry curvatures are only non-zero for non-zero values of α_D, α_R and h_y.

Figure 2 shows the dependence of the anomalous Hall conductivity on the chemical potential μ at zero temperature. The band structure near the origin is shown in the inset. Below $\mu \cong -0.5meV$ there is no contribution to the integral for the anomalous Hall coefficient (see Eq. (2)) as the states near the band gap minimum which have large Berry curvatures (Fig 1) are unoccupied. As μ increases these states are filled and there is a positive contribution to the integral from Ω_-. The quasi-plateau in the hall conductivity for μ corresponds to the energy gap between the two bands where there is a single large Fermi surface away from the origin. It is in this regime

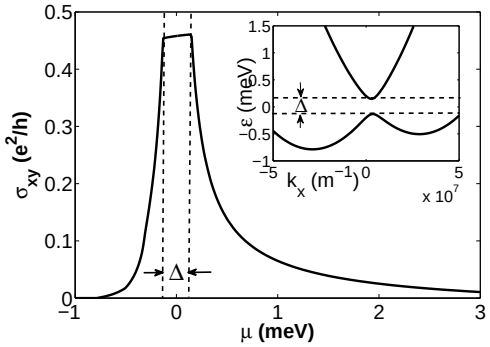

FIG. 2. Anomalous Hall conductivity versus chemical potential μ at zero temperature for a two-dimensional electron-doped semiconductor. We have used $\alpha_R = \alpha_D = 4.74 \times 10^4$ m/s $m^* = .067m_e$ and $h_y = 0.2$ meV. The electronic band structure versus k_x is shown in the inset along with the minimum energy gap Δ indicated by the dashed lines

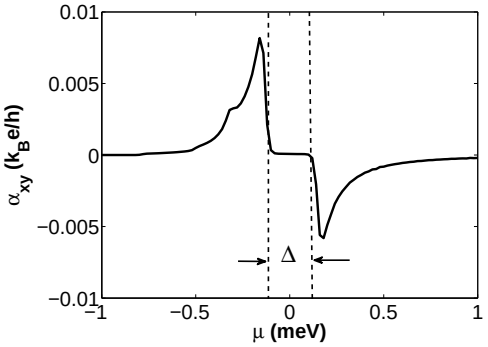

FIG. 3. Anomalous Nernst coefficient versus chemical potential for 2DEG. The dashed lines show the regime of the energy gap Δ between the bands. The same parameters have been used as in Fig 2 with the exception of $T = 0.1K$

of chemical potential that the system supports the topological superconducting state because of the breakdown of the fermion doubling theorem.[12–14,17] At higher μ the upper band becomes occupied, leading to a cancelation of the anomalous Hall conductivity due to the equal magnitude but opposite sign of the Berry curvatures of the two bands.

The anomalous Nernst coefficient for an electron-doped semiconductor near the topological regime is plotted against μ in Fig. 3. At low temperatures the entropy density $s_n(k)$ is sharply peaked at the Fermi surface, such that the integrand in Eq. (4) is non-zero only for values of μ corresponding to the intersection of the Fermi surface(s) and the states near the minimum band gap (close to the origin) where the Berry curvatures are non-zero. Figure 3 illustrates this behavior with a positive peak from the lower band and a negative contribution from the upper band. For the chemical potential slightly below or above the topological regime the system has two (or an even number of) Fermi surfaces one of which lies close to the band degeneracy point. This small Fermi surface, because of a non-zero Berry curvature, gives a finite contribution to the anomalous Nernst effect which differs in sign between the regimes below and above the topological regime. As the topological regime is approached from either side, the Berry curvatures become increasingly sharply peaked (because of a decreasing E_0, see Eq. (6)) while the Fermi surface areas themselves go down resulting in a pair of peaks of opposite signs surrounding the topological regime. The topological regime itself is characterized by a single (or odd number of) Fermi surface with no weight near the band degeneracy points with significant Berry curvatures. Thus, the plateau between the two peaks in Fig. 3 corresponds to the minimum gap separating the energy bands and indicates the regime in which the topological superconducting state is possible.

IV. TOPOLOGICAL HALL AND NERNST EFFECTS IN HOLE DOPED SEMICONDUCTORS

Next we consider thin film hole doped semiconductor quantum wells grown in the [110] direction. In zinc-blende semiconductors the band structure is described by $\boldsymbol{k} \cdot \boldsymbol{p}$ perturbation theory.[45] Here the top valence bands consist of three p-orbitals which have an angular momentum $L = 1$ leading to a six fold degeneracy at the origin. Including spin, the total angular momentum operator becomes $J = L + S$ so that there are four $J = 3/2$ (heavy hole and light hole) and two (split-off) $J = 1/2$ bands which are separated by a large energy gap through atomic spin orbit coupling. We focus on the $J = 3/2$ bands described by the Luttinger Hamiltonian near $k = 0$ which is written as,

$$H_L = \frac{1}{m} \begin{bmatrix} P+Q & -S & R & 0 \\ -S^* & P-Q & 0 & R \\ R^* & 0 & P-Q & S \\ 0 & R^* & S^* & P+Q \end{bmatrix} \tag{7}$$

where the quantities P, Q, R are functions of the Luttinger parameters $\gamma_1, \gamma_2, \gamma_3$ and the momentum components k_x, k_y, k_z and act on the basis $|j, m\rangle$ with $j = 3/2$ and $m = 3/2, 1/2, -1/2, -3/2$ with spin quantization in the growth direction. In Ref. [18] topological superconducting states with a chiral-f-wave symmetry have been shown to exist in hole-doped quantum wells grown in the [001] direction in the presence of a perpendicular Zeeman field and Rashba spin-orbit coupling. A perpendicular Zeeman field, however, is unsuitable for investigations of the anomalous Hall and Nernst effects because such a magnetic field itself gives rise to conventional Hall and Nernst effects which are expected to dominate over the Berry-phase mediated anomalous response. Therefore, in order to uncover the anomalous Hall and Nernst effects in the topological regime of the hole-doped systems, we consider the semiconductor quantum well in the [110] direction with a Dresselhaus spin-orbit coupling and a parallel Zeeman field.

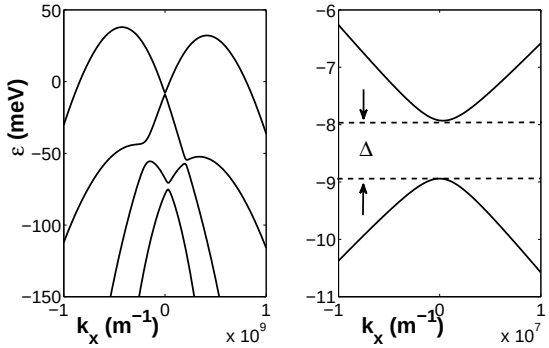

FIG. 4. (a) Band structure of the 2DHG in the k_x direction for $k_y = 0$. (b) Energy gap at origin between lower bands. Here we have used $\alpha_R = \alpha_D = 2 \times 10^5$ m/s, $h_y = 5$ meV, $\gamma_1 = 6.92$,$\gamma_2 = 2.1$, $\gamma_3 = 2.9$ and $a = 8nm$ which are chosen for GaAs.

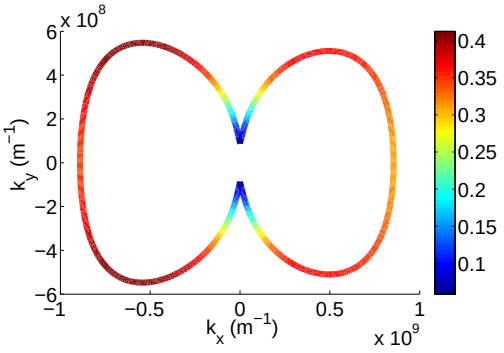

FIG. 5. (Color online) Contour plot of the Fermi surface at μ corresponding to the topological regime ($\mu = -8.5$ meV). Color plot indicates the proportion of light-hole character ($m_j = \pm 1/2$) in the top valence band.

For the [110] growth direction, we have for the functions P, Q, R,[46]

$$
\begin{aligned}
P &= \frac{1}{2}\gamma_1(k_x^2 + k_y^2 + k_z^2) \qquad (8)\\
Q &= \frac{1}{2}\gamma_2(k_x^2 - \frac{1}{2}k_y^2 - \frac{1}{2}k_z^2) + \frac{3}{4}\gamma_3(k_y^2 - k_z^2)\\
S &= \sqrt{3}(\gamma_3 k_x - i\gamma_2 k_y)k_z\\
R &= \frac{\sqrt{3}}{4}((\gamma_2 + \gamma_3)k_y^2 + (\gamma_2 - \gamma_3)k_z^3)\\
&\quad -\frac{\sqrt{3}}{2}(\gamma_2 k_x^2 - 2i\gamma_3 k_x k_y)
\end{aligned}
$$

where we now have k_x, k_y, k_z in the $[0, 0, -1]$, $[-1, 1, 0]$, and $[1, 1, 0]$ directions, respectively. Due to the confinement of the quantum well, the momentum is quantized in the growth direction and is approximated by $\langle k_z \rangle = 0$ and $\langle k_z^2 \rangle \approx (\pi/a)^2$ where a is the width of the well. This confinement projects the above Hamiltonian from three dimensions into two and also serves to lift the degeneracy between the heavy and light hole bands.

The single particle Hamiltonian for a two dimensional hole gas in a [110] quantum well which is expected to support topological superconductivity with s-wave proximity effect is the sum of the Luttinger, spin-3/2 Rashba, and Dresselhaus terms,

$$H = H_L + \alpha_R(\mathbf{J} \times \boldsymbol{k}) \cdot \hat{z} + \alpha_D k_x J_z + h_y J_y \qquad (9)$$

where $\mathbf{J}$ is the total angular momentum operator given by the spin 3/2 matrices, γ_1, γ_2 and γ_3 are the Luttinger parameters, α_R and α_D are the strengths of the Rashba and Dresselhaus couplings and h_y is an in-plane Zeeman splitting as before. The form of the Rashba and Dresselhaus couplings in Eq. (9) for holes can be derived using nearly-degenerate pertubation theory.[45,47] The band structure for this Hamiltonian is illustrated in Fig. 4 with parameters chosen for GaAs. It is clear from Fig. 4 that the combined effects of the Rashba, Dresselhaus, and the in-plane Zeeman splitting give rise to several regimes of the chemical potential where a spectral gap opens up near the band-degeneracy points. In analogy with the electron-doped semiconductors, when the chemical potential falls within the spectral gaps (topological regime) the system has an odd number of Fermi surfaces leading to topological superconductivity in the [110] grown hole-doped well in the presence of superconducting proximity effect.

Next, for a robust s-wave proximity effect on a hole-doped quantum well we need to ensure that the top valence band orbital wave functions couple with the orbitals of the adjacent s-wave superconductor. That this coupling is not automatically assured can be seen from the fact that the valence band holes are generically p-wave (in contrast to the conduction band electrons which are typically s-wave), and therefore coupling with the s-orbitals of the superconductor puts certain constraints on the value of m of the top valence band wavefunctions. To illustrate this, suppose the top valence band quantum state contains contributions only from pure eigenstates of J_z as $\left|j = \frac{3}{2}, m = \pm\frac{3}{2}\right\rangle$. Since $m = m_l + m_s$ where m_l and m_s are orbital and spin angular momentum quantum numbers, respectively, $m = \pm\frac{3}{2}$ implies that this state must consist of only $m_l = \pm 1$, $m_s = \pm\frac{1}{2}$ states. However in this case there will be no overlap between the superconductor orbitals if they are s-wave ($m_l = 0$) and the $m_l = \pm 1$ orbitals of the valence band, and no proximity induced superconductivity can be induced in the valence band. Therefore unlike in the electron conduction band, which consists of s orbitals, we must investigate the orbital angular momentum character of the valence bands for holes.

The eigenstates of the Hamiltonian in Eq. (9) are pure eigenstates of the operator J_z only at $k = 0$, but as k increases the bands become a mixture J_z eigenstates and can be written as a linear combination in the form $|\Phi_n\rangle = c_1(\boldsymbol{k})\left|\frac{3}{2}, \frac{3}{2}\right\rangle + c_2(\boldsymbol{k})\left|\frac{3}{2}, \frac{1}{2}\right\rangle + c_3(\boldsymbol{k})\left|\frac{3}{2}, \frac{-1}{2}\right\rangle + c_4(\boldsymbol{k})\left|\frac{3}{2}, \frac{-3}{2}\right\rangle$. Figure 5 shows the Fermi surface for a value of μ ($= -8.5$ meV) corresponding to the gap between the HH bands (topological regime, see Fig. 4) and the mixing of $m_j =$

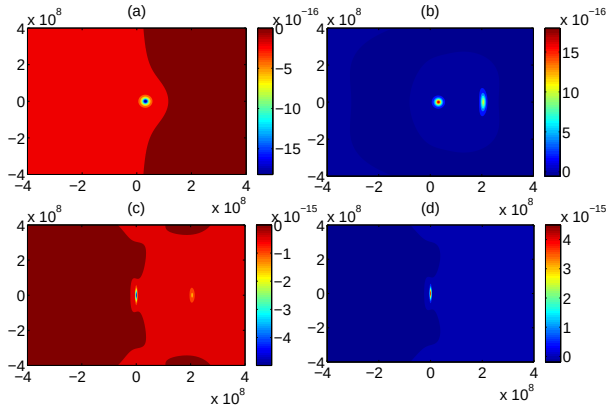

FIG. 6. (Color online) Contour plot of Berry curvature of each band (units of m^2) where (a) corresponds to the lowest band and (d) to the highest. The y and x axis are k_y and k_x respectively with units of m^{-1}. As seen from the denominator of Eq. (10) these functions are sharply peaked at values of $\mathbf{k}$ near the near-band-degeneracy points.

$\pm 1/2$ states given by $|c_2|^2 + |c_3|^2$ in the top band at the Fermi surface. Note that $m_j = \pm 1/2$ eigenstates can be re-written in the basis $|m_l, m_s\rangle$ as a linear combination of $\left|m_l = 0, 1, m_s = \frac{1}{2}, -\frac{1}{2}\right\rangle$ which guarantees the presence of $m_l = 0$ states at the Fermi surface allowing for robust proximity induced superconductivity.

Next we wish to calculate the Berry curvatures associated with the hole band structure shown in Fig. 4 numerically. In order to facilitate the calculations of the Berry curvatures, we use the following expression for the Berry curvature[30] which is equivalent to the form discussed earlier before Eq. (6),

$$\Omega_{xy}^{n} = i \sum_{n' \neq n} \frac{\left\langle \Phi_n \left| \frac{\partial H}{\partial k_x} \right| \Phi'_n \right\rangle \left\langle \Phi'_n \left| \frac{\partial H}{\partial k_y} \right| \Phi_n \right\rangle - (k_x \leftrightarrow k_y)}{(E_n - E_{n'})^2} \tag{10}$$

That this form of the Berry curvatures is equivalent to the earlier expression discussed before Eq. (6) can be understood by noting that $\langle \Phi_n | \nabla_k | \Phi_{n'} \rangle (E_{n'} - E_n) = \langle \Phi_n | \nabla_k H(k) | \Phi_{n'} \rangle$.[30] Eq. (10) has the additional benefit that the arbitrary phase factors of the eigenstates from numerical diagonalization are ignored as there is no differentiation of the eigenstates involved. A contour plot of the Berry curvatures corresponding to each of the four bands is given in Fig. 6. As can be seen from this figure, the Berry curvatures are sharply peaked at points in k-space corresponding to the minimum energy gaps in the band structure of the holes, that is, near the near-band-degeneracy points.

We now calculate the anomalous Hall conductivity through Eq.(2) where we use Eq. (10) for the Berry curvatures, which is equivalent to the Kubo formula in linear response theory. Fig. 7 shows the dependence of σ_{xy} on μ at zero temperature. The physics of this effect is the same as that of the electron doped case but with Berry curvatures and a band structure that are more complicated. Decreasing μ excites more holes, filling each band, such that there are contributions to σ_{xy} corresponding to the overlap of the Fermi distribution function and Berry curvature for each band(Fig 6). As μ is made increasingly large and all bands are filled the sum of the contributions approaches zero. There is again, like in the case of the electron doped semiconductors, a small quasi-plateau corresponding to the topological regime of the chemical potential separating the top two bands.

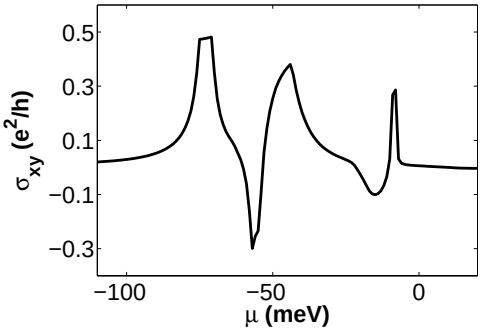

FIG. 7. Plot of the anomalous Hall conductivity for the hole doped semiconductor at T=0 with the same paramaters as those used in Fig. 4.

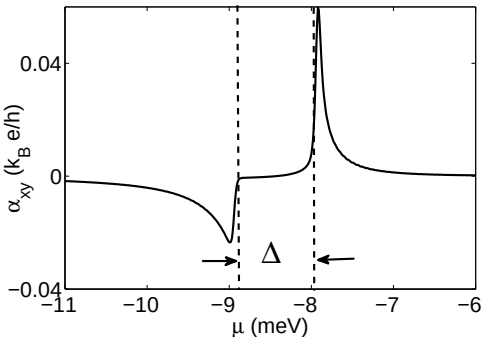

FIG. 8. Plot of the anomalous Nernst coefficient for the [110] grown hole-doped quantum well near the topological regime of the chemical potential. The topological regime of μ is characterized by a plateau of the anomalous Nernst coefficient (at vanishing values) flanked by two peaks of opposite signs as in the case of the electron-doped semiconductors. The parameters used are the same as in Fig. 4 except that $T = 0.1K$.

The regime of chemical potential suitable for topological superconductivity in the presence of s-wave proximity effect can be more clearly seen in the anomalous Nernst coefficient which has a well-defined plateau at vanishing values in the topological regime. We calculate the anomalous Nernst coefficient through Eq. (4) with the Berry curvatures found by using Eq. (10). The μ dependence of the Nernst coefficient is shown in Fig. 8 near the regime of μ near the energy gap Δ between the top bands as illustrated in Fig. 4. Similar to the electron doped systems, the integrand of Eq. (4) is a product of the entropy

density, sharply peaked at the Fermi surface, and the Berry curvatures shown in Fig 6 which are peaked near the near-band-degeneracy points. There are two contributions to Fig. 8 as the Fermi surface corresponding to each band sweeps through the area of k-space near the origin where the Berry curvature is sharply peaked. The plateau for which the coefficient $\alpha_{xy} = 0$ corresponds to the energy gap between the bands which supports the topological superconducting state and is surrounded by well-defined peaks of opposite sign on either side. The vanishing of the Nernst effect, as before, originates from the clear momentum space separation between the single (or odd number of) Fermi surface, which is a requirement for the topological superconductivity with Majorana fermions, and the regions in the momentum space (the near-band-degeneracy points) where the topological Berry phase is sharply peaked.

V. SUMMARY AND CONCLUSION

In this paper we study the intrinsic contributions to the anomalous Hall and thermoelectric coefficients for thin film electron- and hole-doped semiconductors with Rashba and Dresselhaus spin orbit couplings and a suitably directed Zeeman field. Due to the presence of the spin orbit interactions and Zeeman field, a gap is induced in both the conduction and valence bands. When the chemical potential is inside the gap, the so called topological regime, it has been proposed that a topological superconducting state with Majorana fermions may be supported in the presence of s-wave superconducting proximity effect. For the study of anomalous Hall and Nernst effects, we require the applied Zeeman field to be parallel to the planes of the semiconductor. To achieve this, we first introduce the Hamiltonian of a [110] grown hole-doped quantum well and show that in the presence of a parallel Zeeman field several topological regimes of chemical potential open up which can potentially support topological superconductivity in the presence of proximity effect. We then discuss the wave function of the top hole-doped valence band and show that there is a considerable mixing of $m_j = \pm 1/2$ states which is necessary for proximity induced s-wave superconductivity. With the Hamiltonians for the electron- as well as hole-doped systems capable of supporting topological regimes of the chemical potential with only in-plane magnetic fields, we discuss the associated Berry curvatures. Time reversal and spatial inversion symmetry breaking give rise to nontrivial Berry curvatures at the points in k-space corresponding to local minimum gaps between energy bands, the so-called near-band-degeneracy points. We make use of this fact to show that the topological regimes of the chemical potential generically have well-defined plateaus in both anomalous Hall and Nernst effects. While the plateau in the anomalous Hall coefficient is at a non-zero value, the Nernst coefficient saturates in the topological regime at $\alpha_{xy} = 0$. The plateau at $\alpha_{xy} = 0$ is surrounded by well-defined peaks of the anomalous Nernst effect of opposite signs indicating the emergence of the topological regime. The vanishing of the Nernst effect in the topological regime originates from the clear momentum space separation between the single (or odd number of) Fermi surface, a requirement for the topological superconductivity with Majorana fermions, and the regions in the momentum space (the near-band-degeneracy points) where the topological Berry phase is sharply peaked.

VI. ACKNOWLEDGEMENT

This work is supported by DARPA-MTO (FA9550-10-1-0497), NSF (PHY-1104527), DARPA-YFA (N66001-10-1-4025), and NSF (PHY-1104546).

[1] A. P. Schnyder, S. Ryu, A. Furusaki, and A. W. W. Ludwig, Phys. Rev. B **78** 195125 (2008); A. P. Schnyder, S. Ryu, A. Furusaki, and A. W. W. Ludwig, AIP Conf. Proc. **1134** 10 (2009).

[2] A. Yu Kitaev AIP Conf. Proc. **1134** 22 (2009).

[3] S. Ruy, A. Schnyder, A. Furusaki, A. W. W. Ludwig, New J. Phys. **12**, 065010 (2010).

[4] E. Majorana, Nuovo Cimento **5**, 171 (1937).

[5] F. Wilczek, Nature Physics **5**, 614 (2009).

[6] C. Nayak, and F. Wilczek, Nucl. Phys. B **479**, 529 (1996).

[7] N. Read and D. Green, Phys. Rev. B **61**, 10267 (2000).

[8] D. A. Ivanov, Phys. Rev. Lett. **86**, 268 (2001).

[9] A. Stern, F. von Oppen, E. Mariani, Phys. Rev. B **70**, 205338 (2004).

[10] A. Kitaev, Ann. Phys. **303**, 2 (2003).

[11] C. Nayak, S. H. Simon, A. Stern, M. Freedman, S. Das Sarma, Rev. Mod. Phys. **80**, 1083 (2008).

[12] J. D. Sau, R. M. Lutchyn, S. Tewari, S. Das Sarma, Phys. Rev. Lett. **104**, 040502 (2010).

[13] S. Tewari, J. D. Sau, S. Das Sarma, Annals of Physics **325**, 219, (2010).

[14] J. D. Sau, S. Tewari, R. Lutchyn, T. Stanescu and S. Das Sarma, Phys. Rev. B **82**, 214509 (2010).

[15] C. Zhang, S. Tewari, R. M. Lutchyn, S. Das Sarma, Phys. Rev. Lett. **101**, 160401 (2008).

[16] M. Sato, Y. Takahashi, S. Fujimoto, Phys. Rev. Lett. **103**, 020401 (2009).

[17] J. Alicea, Phys. Rev. B **81**, 125318 (2010).

[18] L. Mao, J. Shi, Q. Niu, C. Zhang, Phys. Rev. Lett. **106**, 157003 (2011).

[19] R. M. Lutchyn, J. D. Sau, S. Das Sarma, Phys. Rev. Lett. **105**, 077001 (2010) .

[20] Y. Oreg, G. Refael, F. V. Oppen, Phys. Rev. Lett. **105**, 177002 (2010).

[21] L. Mao, M. Gong, E. Dumitrescu, S. Tewari, C. Zhang, Phys. Rev. Lett. (in press); arXiv:1105.3483.

[22] J. Alicea, Y. Oreg, G. Refael, F. von Oppen, M. P. A. Fisher, Nature Physics **7**, 412-417 (2011).

[23] F. Hassler, A. R. Akhmerov, C.-Y Hou, C. W. J. Beenakker, New J. Phys. **12**, 125002 (2010).
[24] J. D. Sau, S. Tewari, S. Das Sarma, Phys. Rev. A **82**, 052322 (2010).
[25] S. Bravyi and A. Kitaev, Phys. Rev. A **71**, 022316 (2005).
[26] H. Nielssen and N. Ninomiya, Phys. Lett. **130B**, 389 (1983).
[27] A. Y. Kitaev, Physics-Uspekhi **44**, 131 (2001).
[28] M. V. Berry, Proc. R. Soc. London, Ser. A **392**, 45 (1984).
[29] G. Sundaram and Q. Niu, Phys. Rev. B **59**, 14915 (1999).
[30] D. Xiao, M.-C. Chang, Q. Niu, Rev. Mod. Phys. **82**, 1959 (2010).
[31] N. Nagaosa, J. Sinova, S. Onoda, A. H. MacDonald, and N. P. Ong, Rev. Mod. Phys. **82**, 1539 (2010).
[32] D. Xiao, W. Yao, and Q. Niu, Phys. Rev. Lett. **99**, 236809 (2007).
[33] D. Xiao, Y. Yao, Z. Fang, and Q. Niu, Phys. Rev. Lett. **97**, 026603 (2006).
[34] C. Zhang, S. Tewari, V. M. Yakovenko, and S. Das Sarma, Phys. Rev. B **78**, 174508 (2008).
[35] C. Zhang, S. Tewari, S. Das Sarma, Phys. Rev. B **79**, 245424 (2009).
[36] T. Jungwirth, Q. Niu, and A. H. MacDonald, Phys. Rev. Lett. 88, 207208 (2002).
[37] S. Murakami, N. Nagaosa, and S.-C. Zhang, Science **301**,1348 (2003).
[38] Z. Fang, N. Nagaosa, K. S. Takahashi, A. Asamitsu, R. Mathieu, T. Ogasawara, H. Yamada, M. Kawasaki, Y. Tokura, and K. Terakura, Science 302, 92 (2003).
[39] W.-L. Lee, S. Watauchi, V. L. Miller, R. J. Cava, and N. P. Ong, Phys. Rev. Lett. **93**, 226601 (2004).
[40] J. Shi, G. Vignale, D. Xiao, and Q. Niu, Phys. Rev. Lett. **99**, 197202 (2007).
[41] S. Goswami, C. Siegert, M. Pepper, I. Farrer, D. A. Ritchie, and A. Ghosh, Phys. Rev. B 83, 073302 (2011).
[42] A. Dyrdal, and J. Barnas, arXiv:1104.3036.
[43] S.-G. Cheng, Y. Xing, Q.-F. Sun, and X. C. Xie, Phys. Rev. B **78**, 045302 (2008).
[44] Y. Zhang, C. Zhang, Phys. Rev. B **84**, 085123 (2011).
[45] R. Winkler, Spin-Orbit Coupling Effects in Two-Dimensional Electron and Hole Systems (Springer, New York, 2003).
[46] G. Fishman, Phys. Rev. B **52**, 11132 (1995).
[47] L. Mao, M. Gong, S. Tewari, and C. Zhang, to be published.